ORIGINAL PAPER

Additive manufacturing by means of parametric robot programming

Thilo Feucht[1] · Jörg Lange[1] · Maren Erven[1] · Christopher Borg Costanzi[2] · Ulrich Knaack[2] · Benedikt Waldschmitt[1]

Abstract

3D printing or additive manufacturing (AM) is now becoming a common technology in industry. The research activities in this area are constantly increasing, because with the high level of automation and the possibility to produce individual and complex structures, the advantages of additive manufacturing are promising. Most materials used in the construction industry can be used for additive manufacturing, for example steel and concrete. The print head (for example, a welding torch in the AM of steel) is mainly led by industrial robots, whose movements must be transferred from the 3D geometry files to be manufactured. In contrast to all-in-one systems, where hardware, software and printed material are coordinated, most robot-based AM systems are made of components from different manufacturers and branches. The objects to be manufactured are complex and the manufacturing parameters, which significantly influence the geometry and quality of the manufactured part, are manifold. This makes the workflow from the 3D model to the finished object difficult, especially because it is almost impossible to predict the exact manufactured structure geometry or layer height (which would be indispensable for accurate slicing). During the manufacturing process, deviations between the target and actual geometry can occur. In this paper, parametric robot programming (PRP) is presented, which allows flexible motion programming, and a quick and easy reaction to deviations between target and actual geometry during the manufacturing process. Complex geometries are divided into iso-curves whose mathematical functions are determined by means of polynomial regression. The robot can calculate the coordinates to be approached from these functions itself. This allows a simple adjustment of the manufacturing coordinates during the process as soon as target–actual deviations occur. The workflow from the file to the manufactured object is explained. The principle of PRP is transferable and applicable to all robot manufacturers and all conceivable printing processes. In the following article, it will be presented using wire + arc additive manufacturing, in which welding robots or portals can be used to produce steel structures with high deposition rates. Furthermore, the project "AM Bridge 2019" is presented, in which a steel bridge was manufactured in situ over a little creek and the presented PRP was applied.

Keywords Parametric robotic programming · Wire + arc additive manufacturing · On site additive manufacturing · Steel bridge

1 Introduction

1.1 Additive manufacturing in construction industry

Additive manufacturing found its position as an additional tool to manufacture complex geometries or integrate functionalities in components, which were difficult or impossible to be made using traditional or digital controlled subtractive technologies. In addition, AM can be used to improve production chains, for example, by shortening delivery times for spare parts or simplifying logistics in general. The fourth industrial revolution (industry 4.0), which is a collective term for the combination of digitalization, new production methods and automation, aims at production from batch size 1—at the same cost as mass production (Federal Ministry for Economic Affairs 2020). Additive manufacturing is an essential part of this industrial paradigm shift (Lasi et al. 2014). A market study among 560 participants from industry showed that 74% already use additive manufacturing (Vogel Communications Group 2020). The participants, who came from different industries, named the possibility of obtaining innovative product properties, the individualization of the product, but also the shortened production time and cost reduction as the goal of use.

✉ Jörg Lange
  J_Lange@stahlbau.tu-darmstadt.de

1 Institute for Steel Construction and Materials Mechanics, Technical University of Darmstadt, Franziska-Braun-Strasse 3, 64287 Darmstadt, Germany

2 Institute for Structural Mechanics and Design, Technical University of Darmstadt, Franziska-Braun-Strasse 3, 64287 Darmstadt, Germany

Fig. 1 Steel bridge made from WAAM-printed parts (2018)

But 3D printing has not yet landed in the construction industry, which requires long-term reliability, an issue extremely important for buildings with an expected lifespan of 50–100 years, low cost for constructions coupled with a limited development in the craftsmanship, due to low wages and reputation of the industry. However, understanding the potentials for individualization and automation, for building technology and construction industry, a clear trend towards applications can be identified (Buchanan and Gardner 2019).

In the field of building technology and construction research, the most common material (about 80%) being investigated is concrete (Borg Costanzi 2020). Here, the key questions investigated are homogeneity of material, printing processes in speed and dimension, reinforcement technologies and reliability of the material as product (Mechtcherine et al. 2018; Ma et al. 2018; Bos et al. 2016; Buswell et al. 2018). Next to this, the quite broad developed technologies for polymer materials are used intensive, due to the availability and low costs of the technologies (Knaack et al. 2017). Aspects like flammability and limited resistance to UV light are the boundaries. Limited activities can be seen in the field of ceramic materials (Witte and Fehlhaber 2019) and glass (Seel et al. 2018), mainly due to the limited availability of proven AM technologies. Powder-based laser technologies (Strauß 2013; 3DPriyol 2020) for metals are used in the building technology and construction research. Finally, the welding technology-based AM has to be named. With a reliable welding technology, combined with a digitally controlled geometric positioning of the welding device, complex geometrical components can be produced. Recognized actors in the field are the TU Ilmenau/Fachgruppe Fertigungstechnik/Germany, Cranfield University/UK, who branded the acronym "WAAM" and MX3D (Fig. 1), an art, design, and manufacturing company in Amsterdam/The Netherlands (TU Ilmenau 2020; MX3D 2020).

1.2 Robots

The number of robots used worldwide in 2019 amounted to approximately 2.4 million (International Federation of Robotics 2020) and has thus almost doubled since 2013 (International Federation of Robotics 2013). Regardless of the material to be applied, most AM technologies use industrial robots to guide the print head. Robots are better suited for the—usually large—components than CNC machines. Under certain conditions, CNC machines have advantages over robots, especially when high accuracy and post-processing (milling, machining) are required. A major advantage of industrial robots are lower costs, the arbitrary orientation of the print head in space and the possibility—due to their large range of motion—to produce large format structures (Bandari et al. 2015). For example, robots can also be operated on rails, see Fig. 2, which gives them an even bigger range and allows them to add parts directly to large components, which is not possible with closed CNC machines (John et al. 2017).

The project presented in Sect. 3, in which manufacturing was done directly on the construction site, would not have been possible with CNC machines.

1.3 Wire + arc additive manufacturing

Wire + arc additive manufacturing (WAAM) is based on conventional gas-shielded metal arc welding (GMAW) with a filler wire. The wire is the printing material that is applied in line or point by point. This allows the production of three-dimensional structures. The principle of GMAW in the context of WAAM can be seen in Fig. 3.

Compared with other 3D-printing methods using metals—e.g., laser melting or laser sintering—WAAM leads to a significant increase of the deposition rate which is around
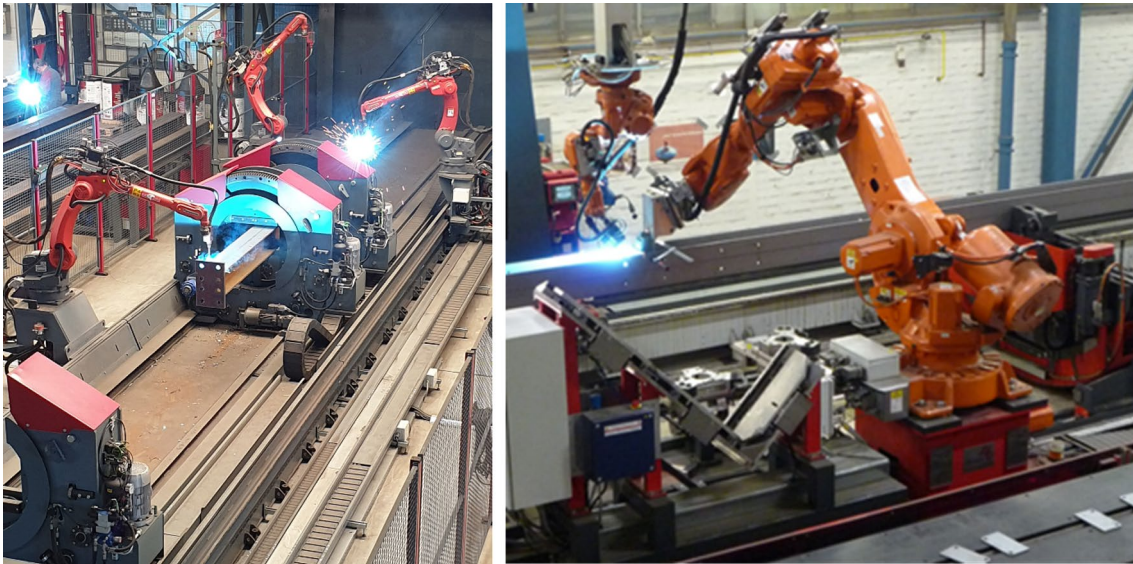
Fig. 2 Automated production lines with handling and welding robots on rails
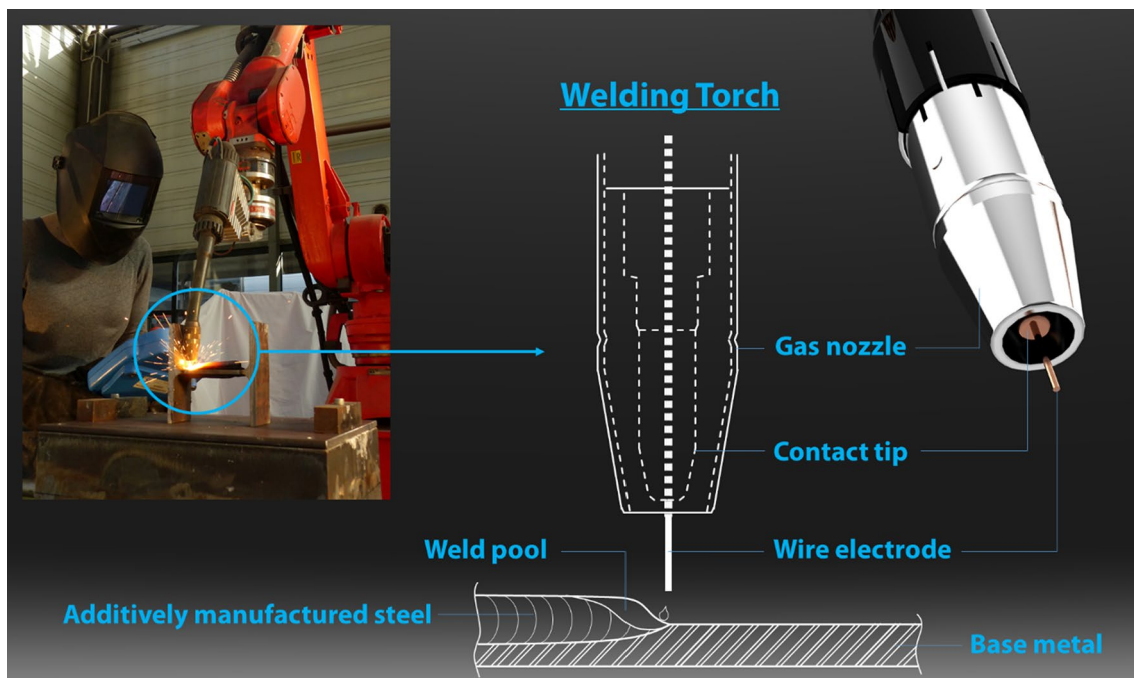

Fig. 3 The principle of GMAW in the context of WAAM

30–40 times more material per time (Bergmann et al. 2018). Furthermore, the cost of WAAM devices (robot and welding equipment) and the material (filler wire) is considerably smaller than for other methods (Martina and Williams 2015) and the powder used in laser technology is very difficult to handle in large-scale industrial application.

In WAAM using GMAW, the filler wire is fed axially through the contact tip of the welding torch. As soon as the wire touches the component, a short circuit with an electric arc develops. This leads to temperatures of more than 10,000 °C and the wire melts. At this temperature, the fused material is prone to corrode and therefore, a gas shield has to prevent the reaction with oxygen or other corrosive components. Usually, a little bit of molten metal drops off interrupting the short circuit. This happens with frequencies of up to 130 Hz (Fronius et al. 2013). With each arc ignition,

Fig. 4 Two different strategies to manufacture a layer (Ding et al. 2014)
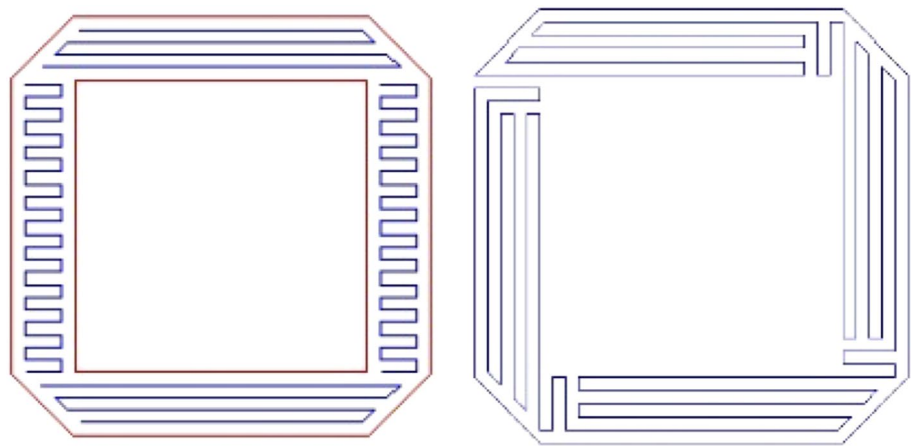
small volumes of the component and previously deposited drops melt. If the welding torch is not moved, the size of the drop increases (spot welding). Otherwise, a weld seam is developed.

The material deposition of conventional 3D printers using plastic filaments and of WAAM is alike, and leads to small bulges. However, filler wire has a far smaller viscosity than common 3D-printer filaments of thermoplastic polymers [mostly polylactides (PLA)], increasing the problem of producing a stable geometry. The magnitude of the viscosity, the cooling velocity and, therefore, the solidification of the molten metal are decisive for the geometry and the material characteristics of the weld seam. The factors that influence the geometry and the material characteristics are manifold and are listed below.

Input parameters.

- Wire electrode
- Wire diameter
- Shielding gas
- Gas flow rate
- Geometry of the gas nozzle
- Welding system

Process parameters.

- Current
- Voltage
- Wire feed speed
- Welding process regulation (e.g., standard, pulse)
- Travel speed

Thermal boundary conditions.

- Interpass temperature
- Temperature history/temperature cycles
- Cooling

Geometric boundary conditions.

- Orientation of the nozzle (neutral, dragging, piercing).
- Welding position (trough position, rising, falling).
- Contact tip to work distance (CTWD).
- Weld seam beginning, weld seam center, weld seam end.

1.4 Slicing and manufacturing strategy

Since model-based robot programming is replaced by parametric robot programming both are described below with their reference to the slicing process.

Slicing is the process of partitioning the final geometry into layers or dots onto which the material has to be deposited. The layers are described by movement commands (mostly linear or circular) and coordinates.

Conventional 3D printer usually use the so-called G-Code, which is also used for common machine control. Existing slicing software generates the layers and the G-Code for common printers automatically.

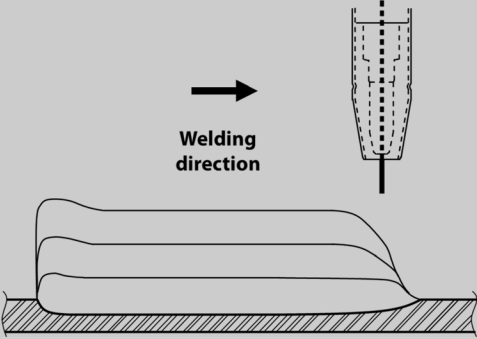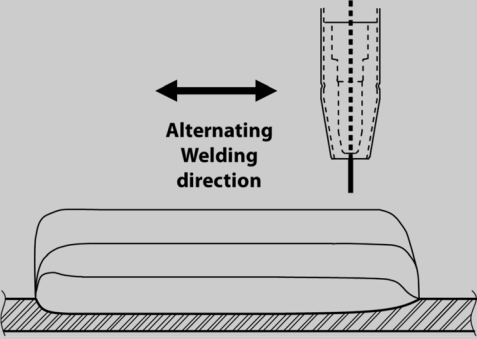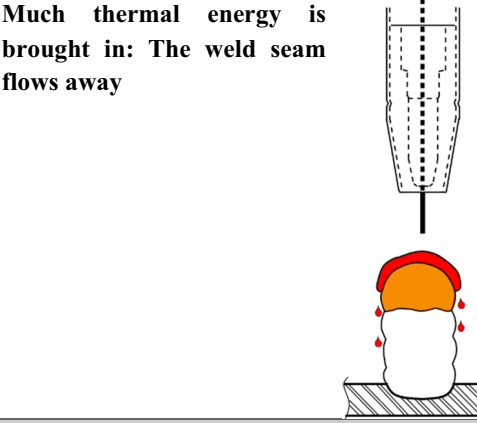Depending on the final geometry, various possibilities and strategies of slicing are possible, see Fig. 4.
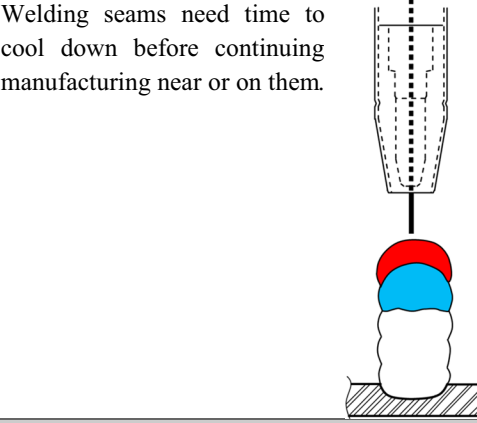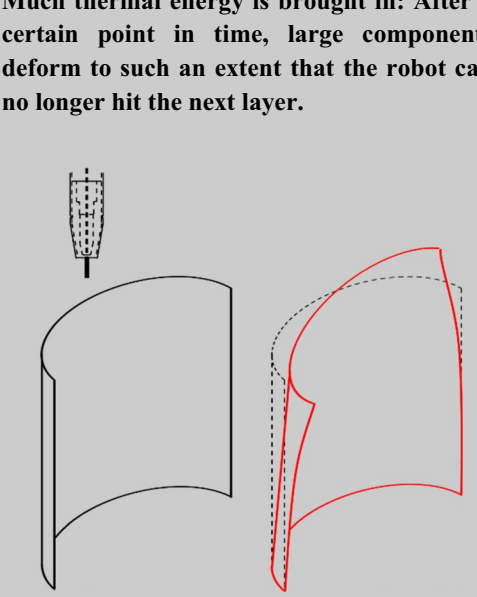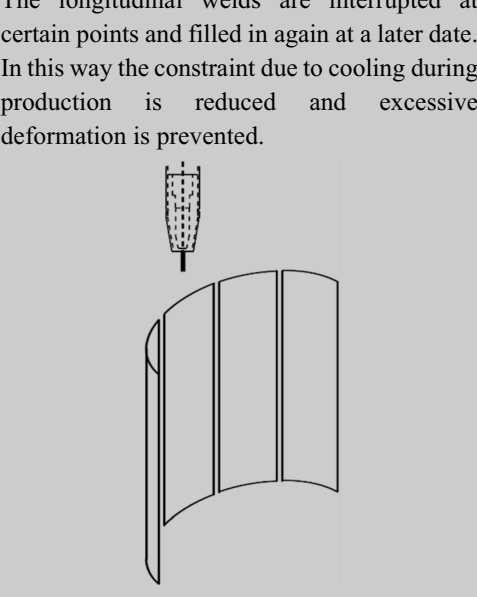
Widely used slicer programs, e.g., Slic3r,[1] offer various setting options that can be used to partially influence the slicing and the manufacturing strategy. The experience of the authors shows that components that are suitable for the construction industry cannot be adequately sliced. Especially for WAAM, such slicers are not appropriate due to its particularities.

Some of these particularities are listed in Table 1.

Each additive-manufactured material has its own peculiarities. For example, in the additive manufacturing of clay, it must be taken into account during slicing that shrinkage occurs due to baking.

---

[1] https://www.slic3r.org/.

Table 1 Chosen particularities of the WAAM

	Particularity	Aspiration
1	**At a constant speed, welds are higher at the starting point and lower at the end point than in the rest area ([25]). These different heights can accumulate.**	For example for wall-like structure with linear material deposition, it is advantageous to alternate the welding direction, i.e. to change after each layer.
2	**Much thermal energy is brought in: The weld seam flows away**	Welding seams need time to cool down before continuing manufacturing near or on them.
3	**Much thermal energy is brought in: After a certain point in time, large components deform to such an extent that the robot can no longer hit the next layer.**	The longitudinal welds are interrupted at certain points and filled in again at a later date. In this way the constraint due to cooling during production is reduced and excessive deformation is prevented.

With the WAAM, there are always different possibilities in which way the structure can be built. The definition of the procedure, e.g., in which order and in which direction the layers are applied is called manufacturing strategy. Row 3 of Table 1 shows two different production strategies. Both theoretically lead to the same geometry, but the left strategy is problematic and, therefore, the right strategy is preferable. The choice of the proper strategy has to do with the experience of the operator and the knowledge of suitable strategies and, therefore, cannot be decided by a software (at least not yet).

To ensure that the layers will add up to the aspired structure, the form of each weld must be known prior to the fabrication. Fundamental for the shape of each weld are the traveling speed of the printing head (in case of WAAM the welding torch) and the amount of the extrusion (in the case of WAAM the wire feed speed is taken as a parameter). Information on the movement, beginning and end of the extrusion, the various speeds, etc. are converted into program code for the printer.

An accurate prediction of the geometry is necessary but because of the many parameters (listed above) difficult. Therefore it seems reasonable to create a feedback loop from the geometry of the actually fabricated weld seam to the planning of the subsequent weld seam. A deviation of the target to the actual value can lead to an interruption of the manufacturing process. It might lead to visual failures by reason of too large or small CTWD, or to an arc start failure. In model-based robot programming after detection of deviations in the as-built geometry, it is obviously necessary to pass through a new slicing procedure including the calculation of a new G-Code. This is particularly complicated if the slicing is not directly linked to the robot and is performed as a separate upstream process (which is very common due to the complexity of linking all processes).

Figure 5 shows the deviation of nominal to actual layer height Δz, which leads to a larger electrode extension (CTWD). Since a change of the electrode extension leads to a change of the layer geometry (Almeida 2012), new slicing is necessary—and this might occur several times.

Using the newly developed robot programming described hereafter, these additional feedback loops and all associated additional operations can be omitted. This is because in case of PRP, the geometry to be manufactured has already been completely described via the parametric robot code. Only the actual height has to be measured and transferred to the robot, so that it can automatically recalculate the required x- and y-coordinates.
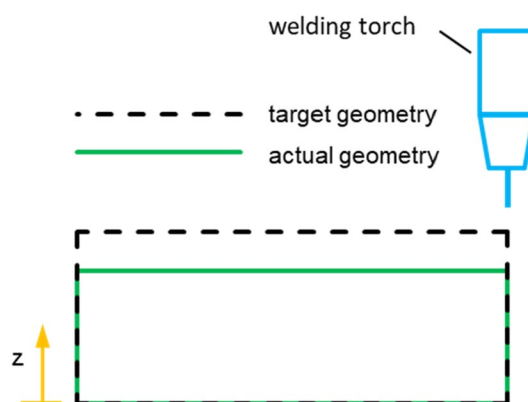

Fig. 5 View of a wall-like structure

Fig. 5 View of a wall-like structure

2 Parametric robot programming

In parametric robot programming, the geometry of the structure that shall be fabricated is described by mathematical functions. x- and y-coordinates are functions of the z-coordinate:

$$x = f(z), \quad y = f(z).$$

The orientation of the welding torch is defined by the angles a, e and r (Euler angles), and might also be defined depending on z:

$$a = f(z), \quad e = f(z), \quad r = f(z).$$

This allows to react quite flexibly on deviations between target and actual geometry. No explicit coordinates have to be given to the robot but only the mathematical functions and the z-coordinates. The functions can be used for the determination of the geometry (see upcoming section). Very complicated geometries can also be described by functions, e.g., using polynomial regression (see also Sect. 2.2.2).

The parametric robot programming allows to start the fabrication even without the knowledge of single layer heights. After producing the first layer, the actual geometry is identified, the z-coordinate is transferred to the robot controller and further x- and y-coordinates are calculated. The assessment of the actual geometry and the comparison between actual and nominal geometry can be made in accordance with the available surveying tools and previously defined termination criteria. The team at TU Darmstadt uses the "Touch Sensing Method". Therefore, the filler wire is cut by
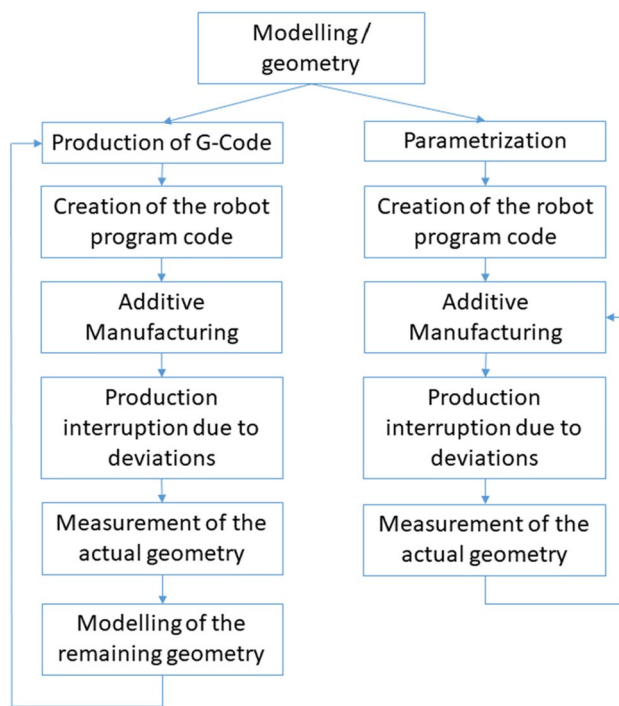
Fig. 6 Comparison of the model-based and the parametric programming of robots in WAAM

a wire cutting station to a defined length automatically and a small voltage is applied. By slowly moving the wire onto the workpiece, the coordinates of the point where the wire touches the workpiece (and the electric current flow starts) are recorded by the robot. The now known coordinate can be processed further, for example, its z-coordinate can be used to calculate the x- and y-coordinates required for the next layer. On the basis of experience with regard to the prediction of the geometry, the surveying frequency is defined after every second layer.

The procedures of conventional slicing (model-based) and parametric robot programming are compared in Fig. 6.

2.1 Simple structures

In this section, the parametric programming of robots shall be described using simple examples in which the functions were chosen in advance.

2.1.1 Linear wall structures

Figure 7 shows a wall which is characterized by a constant y-coordinate. Therefore, only the x-coordinate has to be defined. The fabrication demands that the robot leads the welding gun from point 1 to point 2. The x-coordinates of these two points depend on z. Point 2 is part of an ellipse.

The production can be programmed using a conventional FOR loop, which is explained in detail below. The parameterized robot code is listed as follows.

```
z = 0, Δz = layer-height, h = total height, Δx₁, Δx, Δx₂ = parameters (arbitrary)
FOR i = 1 TO 999 DO
        x₁ = z · Δx₁ / h
        x₂ = Δx1 + Δx + Δx₂ / h · (h² - z²) ^ (1 / 2)
        Point1.x = x1
        Point2.x = x2
        MOVE LINEAR TO p1
        arc_start
        MOVE LINEAR TO p2
        arc_end
        MOVE LINEAR AWAY 20 ADVANCE
        z = z + Δz
        Point1.z = z
        Point2.z = z
        IF z >= h THEN
                i = 999
        ENDIF
ENDFOR
```

Fig. 7 View of the wall in para-
metric definition including the
functions of the beginning and
end of the welding process

$$f_1(z) = z \cdot \Delta x_1/h$$
$$f_2(z) = \Delta x_2/h \cdot \sqrt{h^2 - z^2}$$
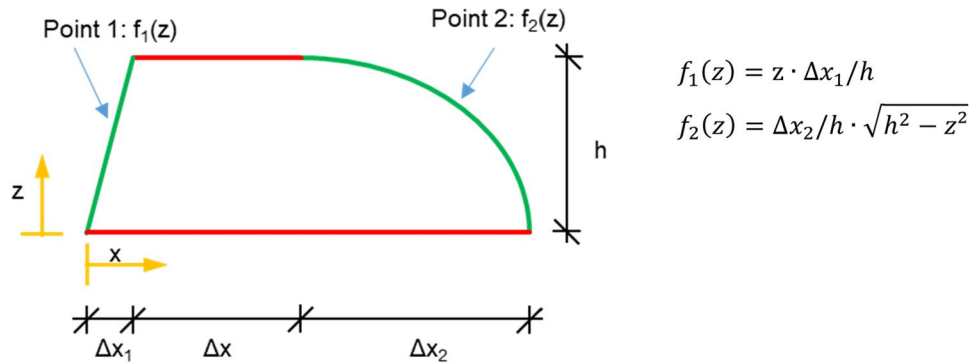
2.1.2 Linear volume

A further example might be a jar, as given in Fig. 8a. A structure like this might be used as a column head (Fig. 8b) to allow a new beam layer under a certain rotation towards the lower beam layer.

In this case, the jar is a pentagon increasing its side length over the height and rotating its sides also depending on the height. With parametric programming, the same code may be used for a square. In this case, the parameter for the number of angles would have to be changed from 5 to 4. The correlation is given in Fig. 9.

Usually, the starting point (centre of the circumscribing circle) is transferred to the robot. The points creating the final structure (in this case the pentagon) are calculated depending on the "number of angles" and the radius "r" of the circle. If the centre of the circle is given in an existing coordinate system, all further coordinates result from a difference between starting and end point, which is shown in the following example. It might be reasonable to locate the coordinate system on the starting point, which will make all coordinates to absolute values. Both approaches have advantages and disadvantages.
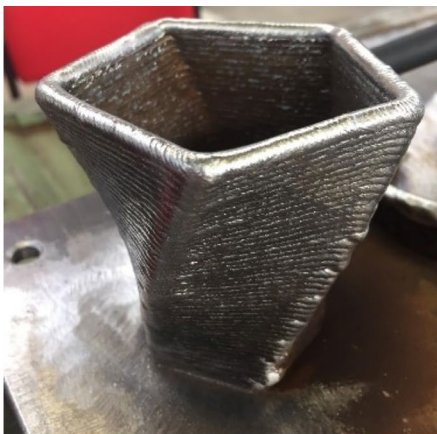
As can be seen in Fig. 8a, the diameter of the circumscribing circle increases with the height. This can be programmed by describing the radius "r" with function of "z". This was a linear function, with R_u being the radius on bottom and R_o on top the function is:

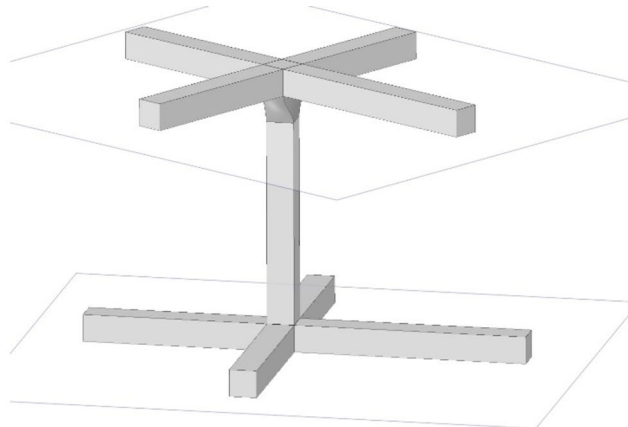$$r(z) = R_u + ((R_o - R_u)/H) \cdot z.$$

In this case, it is important to consider the possible overhang of the seam to avoid the loss of material by dripping off. Furthermore, a rotation of the pentagon was programmed. The rotation angle "d" was also depending on "z". In the example given in Fig. 8a, every 10 mm, a rotation of 4° was defined leading to:

$$d(z) = 0.25 \cdot z.$$

The structure is defined by two loops. The first refers to the layers. Within this loop, a second loop defines the points according to the cross section which was defined. After closing the second loop, the height can be identified and the coordinates of the next layer will be calculated according to the result. The code is given below.

(a)

(b)

Fig. 8 Column head

$$\alpha = \frac{360°}{\text{number of angles}}$$

for 5 Points

$$\alpha = \frac{360°}{5} = 72°$$

Point ① : $\varphi = 0$

x − coordinate: $r \cdot \sin(\varphi) = 0$

y − coordinate: $r \cdot \cos(\varphi) = r$

Point ② : $\varphi = 72° = 1 \cdot \alpha$

x − coordinate: $r \cdot \sin(\varphi) = 0{,}95 \cdot r$

y − coordinate: $r \cdot \cos(\varphi) = 0{,}31 \cdot r$

Point (i) : $\varphi = (i - 1) \cdot \alpha$

x − coordinate: $r \cdot \sin(\varphi) = r \cdot \sin((i - 1) \cdot \alpha)$

y − coordinate: $r \cdot \cos(\varphi) = r \cdot \cos((i - 1) \cdot \alpha)$
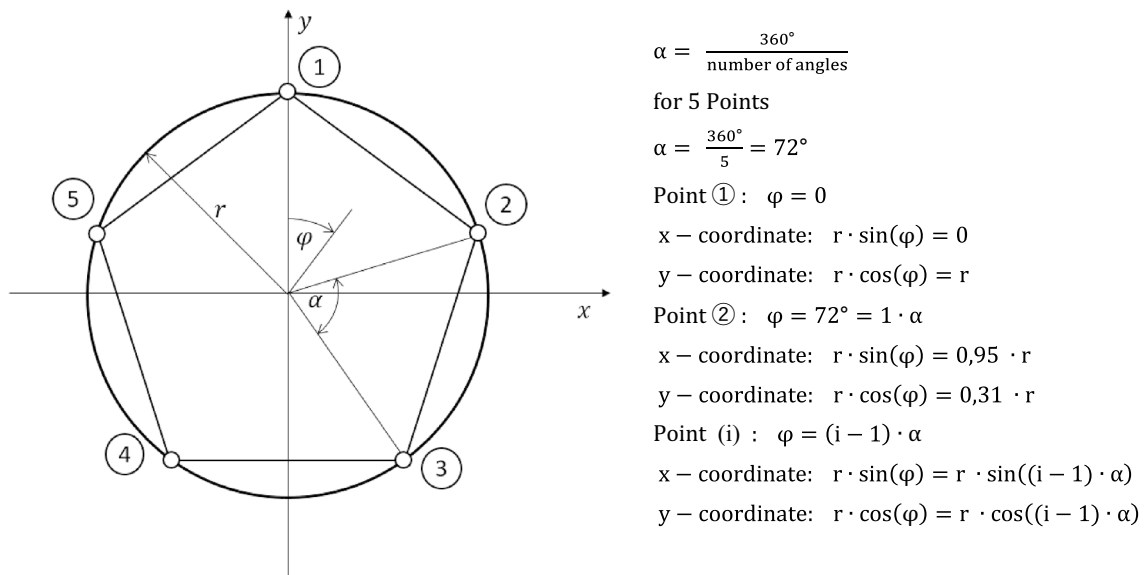
Fig. 9 View of the jar in parametric definition including the functions of the beginning and end of the welding process

```
p0 := POS(x0, y0, z0, a0, e0, r0)  -- Middle
z := 0; Number := 5; alpha := 360/Number;  Ru := 25; Ro := 50 ;  H := 100; lmax := 40  -- parametric variables

  FOR l := 0 TO lmax - 1 DO
          r := Ru + (Ro - Ru) / H * z
          d := 0.25 *z

          FOR i := 1 TO Number DO
                  point[i] := POS(x0 + r * COS((i - 1) * alpha + d), y0 + r * SIN((i - 1) * alpha + d), z0 + z, a0, e0, r0)
          ENDFOR

          MOVE LINEAR TO point[1]
          arc_start(29)
          arc_job(29)
          FOR i := 2 TO Number DO
                  MOVE LINEAR TO point[i]
          ENDFOR
          MOVE LINEAR TO point[1]
          arc_end(1)
          MOVE LINEAR RELATIVE VEC(0, 0, -100) IN TOOL

          h := 2
          z := z + h
  ENDFOR
```

Only this number of code lines is necessary to give all information that is needed for the robot. No dependency on the height of the structure is given. This means whether it is 10 cm or 50 cm high, the same number of code lines is needed. The advantage of parametric programming can be seen in Fig. 10. This structure is 10 cm high. Assuming that each layer has a height of 2.5 mm, 40 layers will be needed. With five points for each layer, 200 points have to be given in conventional code. Parametric programming transmits this information using only four functions.

Furthermore, the parametric code can react to differences in the manufactured height. If the assessment of the layers gives, for example, the result that their height is only 1.5 mm, the conventional code has to be recreated and will lead to 330 points. In the parametric code, the height "z" and the thickness of the seam "h" will be adjusted, leading continuously to correct coordinates.
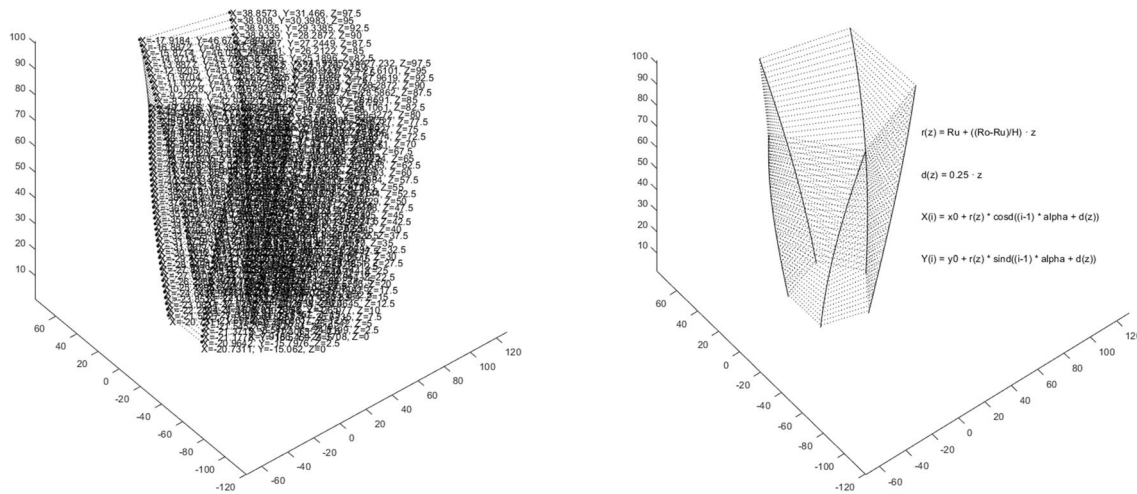
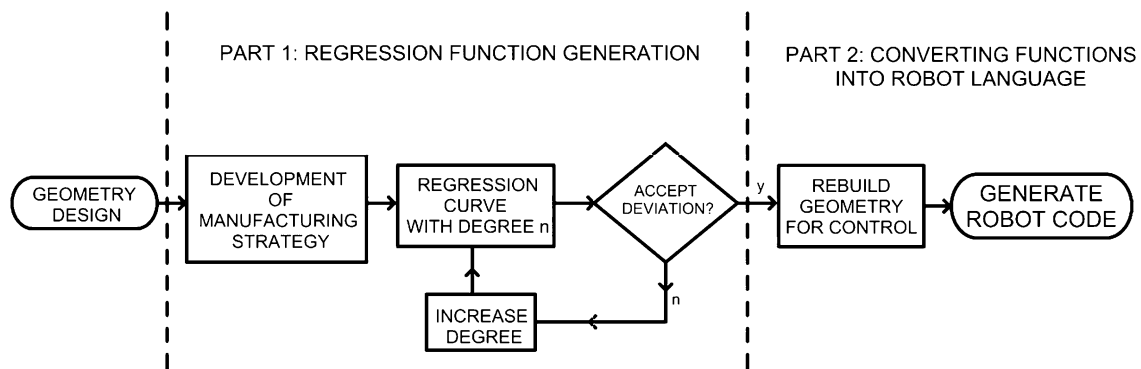**Fig. 10** Example for conventional code (left) and parametric programming (right)

Fig. 11 Workflow for parametrization of the geometry

2.2 Complex structures

The structures presented in the previous paragraph result from known functions. However, one of the greatest advantages of additive manufacturing is that structures are feasible even when they are defined by complex mathematical functions. Their geometry might be the result of structural optimization or other processes. An example for this will be given in Sect. 3.1.

For these complex structures, a workflow was developed to utilize the advantages of parametric robot programming. This workflow (Fig. 11), which combines various known processes in a new way, and its special aspects to be considered will be explained in the following section.

2.2.1 Preprocessing

When having a 3D geometry to be printed, thoughts of how it should be printed are needed. Besides the normal aspects of slicing in 3D printing, e.g., smooth surface, equal thermal impact (see also Sect. 1.4), for Parametric robot programming, some more have to be considered as well.

- What should be the controlling variable?
- Where is the appropriate coordinate system?
- Has one controlling variable just one resulting variable per function?

For the controlling variable, which means that variable which gives a feedback about the printed structure and is used to calculate the further structure, often the z-coordinate is used (e.g., Sects. 2.1.1 and 2.1.2). Especially, when printing in neutral position, it is a reliable feedback of the ongoing process and the already printed structure (see Sect. 1.4, Fig. 5). However, when the printing orientation is changed (as is common within WAAM), the structure must be divided into sections, each having its respective reference frame. With a local coordinate system for this part new functions can be found referring to the z-coordinate or another reasonable controlling variable. For the here-shown parametric programming, ordinary polynomial functions are used (e.g. Sect. 2.2.2); thus, the structure has to be split in parts such that each rebuilt curve just has one result for one
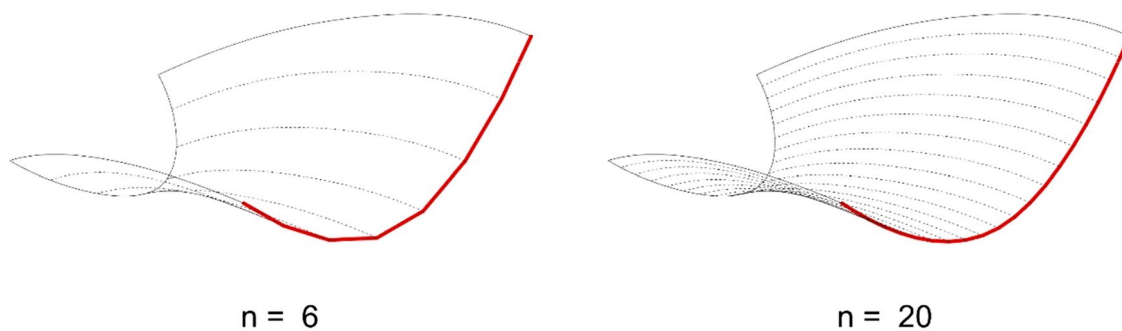
n = 6   n = 20

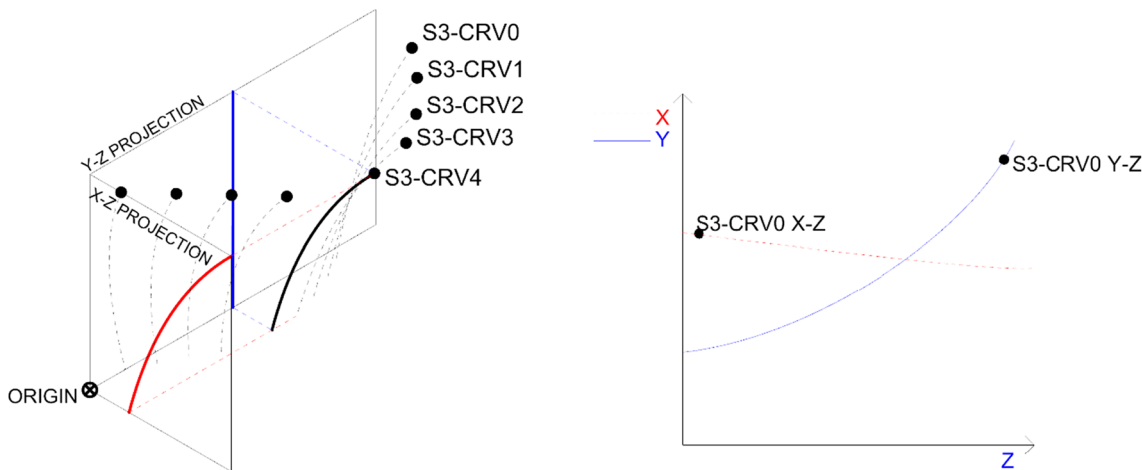**Fig. 12** Reconstruction of a surface by iso-curves

Fig. 13 Projection of iso-curves onto *x–z* and *y–z* planes

controlling variable value. After developing a manufacturing strategy for the geometry, an example is shown in Sect. 3.2, each part of the geometry can be defined by polynomial functions, as described in the following sections.

2.2.2 Finding of the polynomial regression

Polynomial regression is a form of regression analysis commonly used for determining a best-fitting curve through data points to establish a mathematical equation which best estimates the data set (Brandt 2014). In this research, a dataset is provided by dividing iso-curves into a number of points. A polynomial regression tool available on MathNet (Math. NET Numcerics 2020) is used in combination with parametric design software, Grasshopper 3D, to calculate the polynomial function which describes the best-fit curve of each dataset.[2] The tool calculates the polynomial function of the given division points as the following general equation:

$$\rightarrow a_1 + a_2 x_i + a_3 x_i^2 + \cdots + a_n x_i^{n-1} = y_i \quad \text{for } (i = 1, \ldots, n).$$

To describe a non-arbitrary geometry in terms of mathematical functions, it is rebuilt first as a series of its iso-curves. The extracted curves are subsequently described as their polynomial function and reconstructed as a 3D geometry.

The density of the iso-curves used to define the geometry has a direct effect on the reconstructed shape: a lower number of curves results in a higher kink angle between sections. As the number of iso-curves increases, the kink angle is decreased and the reconstructed geometry approximates a more curved section (Fig. 12). A fitness function is used to minimize the amount of iso-curve divisions needed to obtain a reconstructed geometry which best approximates the original shape.

To obtain the mathematical functions of the divided geometry, the three-dimensional iso-curves must be reduced to planar curves, allowing for curves to be expressed separately in terms of both $f(z) = x$ and $f(z) = y$ functions. This is achieved by projecting each curve onto their respective *x–z* and *y–z* planes (Fig. 13).

An evolutionary algorithm tool (Galapagos[3]) is used to optimize the distribution of initial division points such that

---

[2] Other regression methods or programs can also be used.

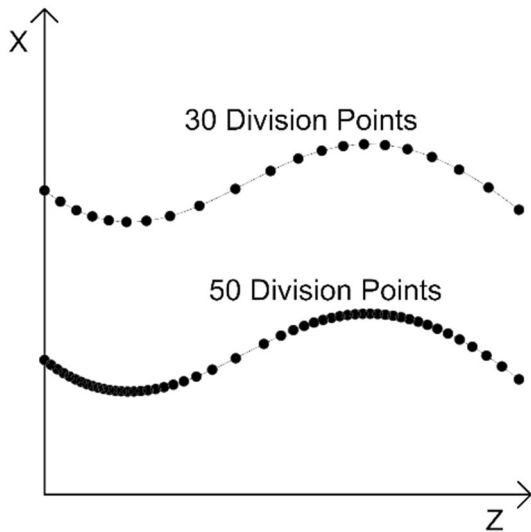[3] Other methods or programs can also be used.

Fig. 14 Variation of distribution point density to achieve best-fit solution

the polynomial with the lowest degree and lowest deviation from the original curve (the nominal geometry) is achieved (Figs. 14, 15).

2.2.3 Rebuilding geometry for control

Once all the functions for each curve projection are determined, they are exported as a list to MATLAB for control.

Since all functions are identified separately and uncoupled from the structure, a downstream process produces a model that represents the structure given by the functions and this would be printed finally. Comparing the nominal geometry with this model the quality of the functions can be assessed. Figure 16 presents an example.

Figure 16a illustrates the geometry which shall be printed as well as one of the areas (surface marked in red). Once the functions are determined for each segment, they are re-simulated as a complete 3D model (Fig. 16b) and assessed on whether they have been accurately determined. There are numerous reasons why incorrect 3D models may occur; under- and over-fitting of polynomial regression curves may happen when too few or too many polynomial degrees are used. In this case, the degree is increased or decreased and functions are found once more. Errors may also occur due to malfunctions in the script for calculating functions or too few significant digits are used in the functions. When such errors occur, they are adjusted for the points mentioned above and re-generated to achieve a better-fitting curve (Fig. 15). This example proofs vividly how important a downstream examination is.

Fig. 15 Variation of curve degree to achieve best-fit solution

(a) Nominal geometry   **(b)** Model with wrong functions   **(c)** Model with correct functions
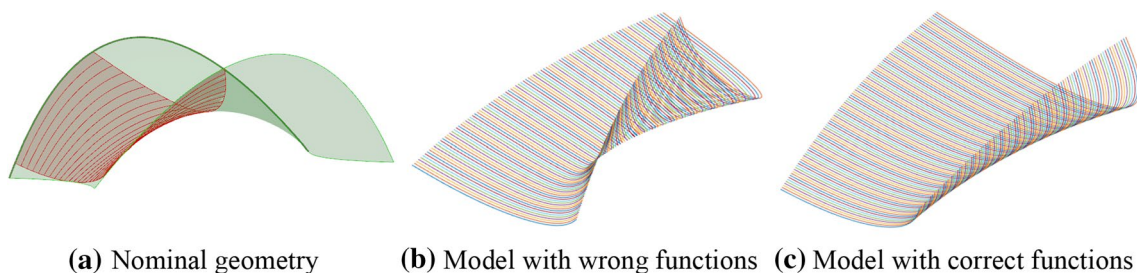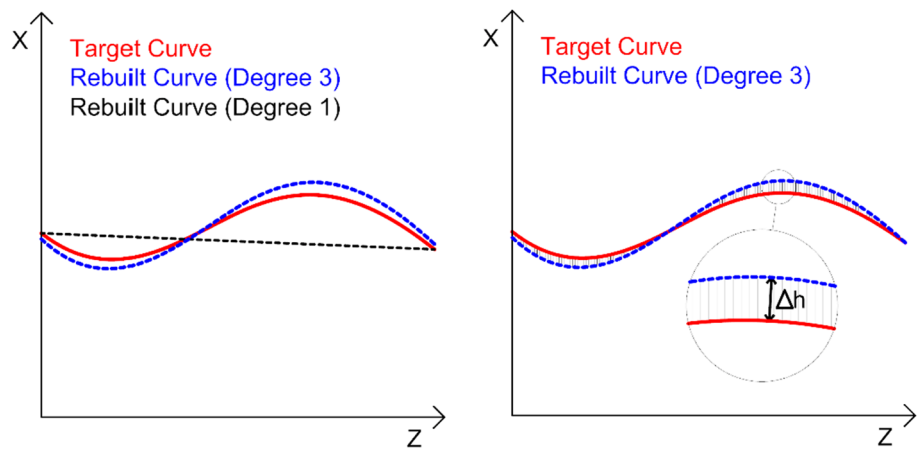
Fig. 16 Nominal geometry and representations

2.2.4 Development of the code for the robot

If the geometry produced by the functions is within an acceptable range of variation with the nominal geometry, the functions may be used by the robot. The code can be generated from the functions automatically.

The developed functions $f_1(z) = x$ and $f_2(z) = y$ for the iso-curves represent the course of one point over the height z in space. The number of functions per point defines the number of position variables needed, e.g., as mentioned in Sect. 2, the orientation of the robot can also be parametrized. Connecting the points of several functions at a constant z-height now gives the weld path for a layer.

These points are declared as position and initialized by (x, y, z, a, e, r) with starting values. Within a loop, the x- and y-coordinates are calculated using the functions for the actual z-height and the welding is performed. In the end of one loop run the z-height increases and is used for calculating the coordinates in the next loop run. Instead of the enormous number of points of the whole structure only the points that are needed for the welding will be calculated. After each layer it is possible to adjust the height, a great advantage of the parametric programming.

An excerpt of such a program code (PDL language for Comau robots) is shown below:

Fig. 17 Picture from construction site

3 Project "AM Bridge 2019"

The previously explained workflow was developed for the project "AM Bridge 2019", where a steel bridge was printed in situ across a creek, see Fig. 17.

```
point[1] := POS(0,0,0,0,0,0)
point[2] := POS(0,0,0,0,0,0)
...
point[20] := POS(0,0,0,0,0,0)
z := 0
lmax := 100

FOR l:=0 to lmax do
        point[1].x := (320.97874) + (-0.28095) * z + (0.000036) * z**2
        point[2].x := (359.76736) + (-0.25041) * z + (0.000027) * z**2
        …
        point[20].x := (508.51215) + (-0.17848) * z + (0.000017) * z**2

        point[1].y := (1251.37726) + (-0.13718) * z + (-0.000171) * z**2
        point[2].y := (1202.52922) + (-0.13581) * z + (-0.000191) * z**2
        …
        point[20].y := (1051.20588) + (-0.17492) * z + (-0.000232) * z**2

        move linear to point[1]
        arc_start(1)
        arc_job(1)
        FOR i:=2 TO 20 DO
                move linear to point[i]
        ENDFOR
        arc_end(1)
        move away 200

        h:= 2.5
        z:=z+h
ENDFOR
```
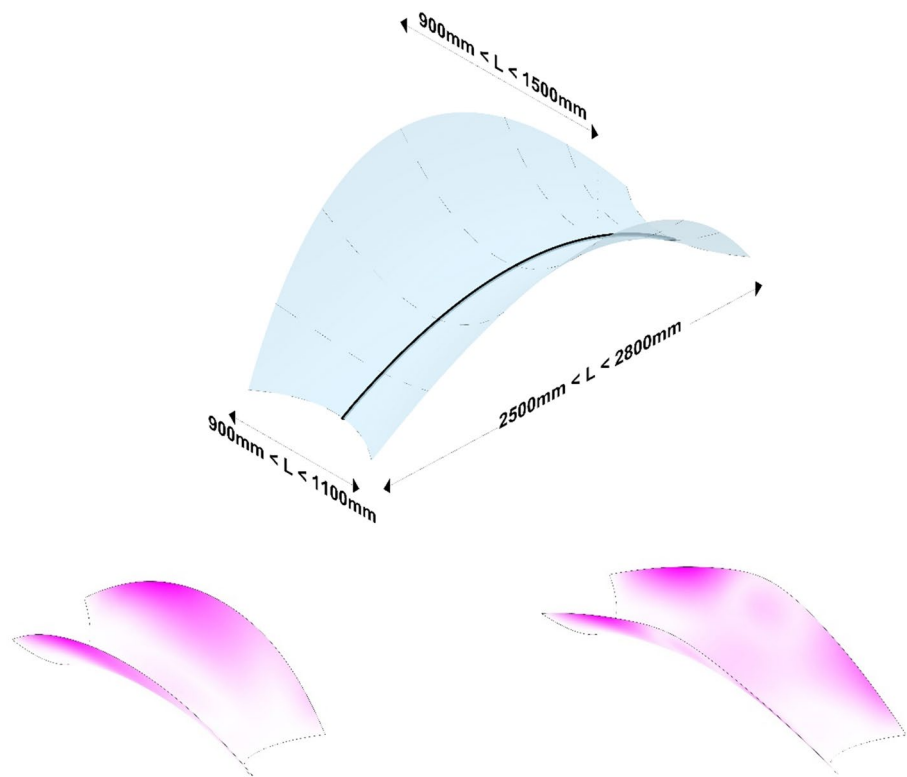
Fig. 18 Form-finding model in Grasshopper

In the following, the form finding, the development of the manufacturing strategy and the characteristic of the project are explained.

3.1 Form finding

Generating the geometry of the bridge begins with fitting the form finding model onto a 3D scan of the printing site. A Faro Focus 3D laser scanner was used to scan the area and generate a mesh/point cloud onto which the form finding model was superimposed. The exact parameters for starting angles and span are extracted from the mesh and used to define the boundary conditions for generating the final design.

To test the adaptability of the parametric functions to construction elements, a pedestrian bridge structure was designed. The geometry of the structure is the result of an iterative form finding process using Rhinoceros 3D and the plugins Grasshopper 3D and Karamba. This allows for the geometry to be designed for the ideal structural shape and easily adapted to different sites. The final design object was chosen using multiple-objective optimization which had to meet the following design criteria:

- Design which gives minimum deflection under self-imposed load.
- Design which gives minimum elastic energy under self-imposed load.

- Design with smallest surface area and hence overall weight.

With the following design constraints (Fig. 18):

- Overall span between 2500 and 2800 mm, to remain in bounds of robot reach.
- Widths of 900–1100 mm at entrance, and midspan width not larger than the entrance width and smaller than 1500 mm due to robot reach limits.

Octopus, an evolutionary solver for Grashopper 3D, was used to generate a set of design options which satisfied the above-mentioned criteria. A number of "best-fit" results were extracted and the final shape was chosen based on aesthetic criteria.

3.2 Manufacturing strategy

The following manufacturing strategy was applied. The bridge was divided into segments in which different manufacturing directions or layer divisions were used. The segments are symmetrical for each bridge side and can be seen in Fig. 19. They then were divided into 100 iso-curves whose polynomial functions were determined using linear

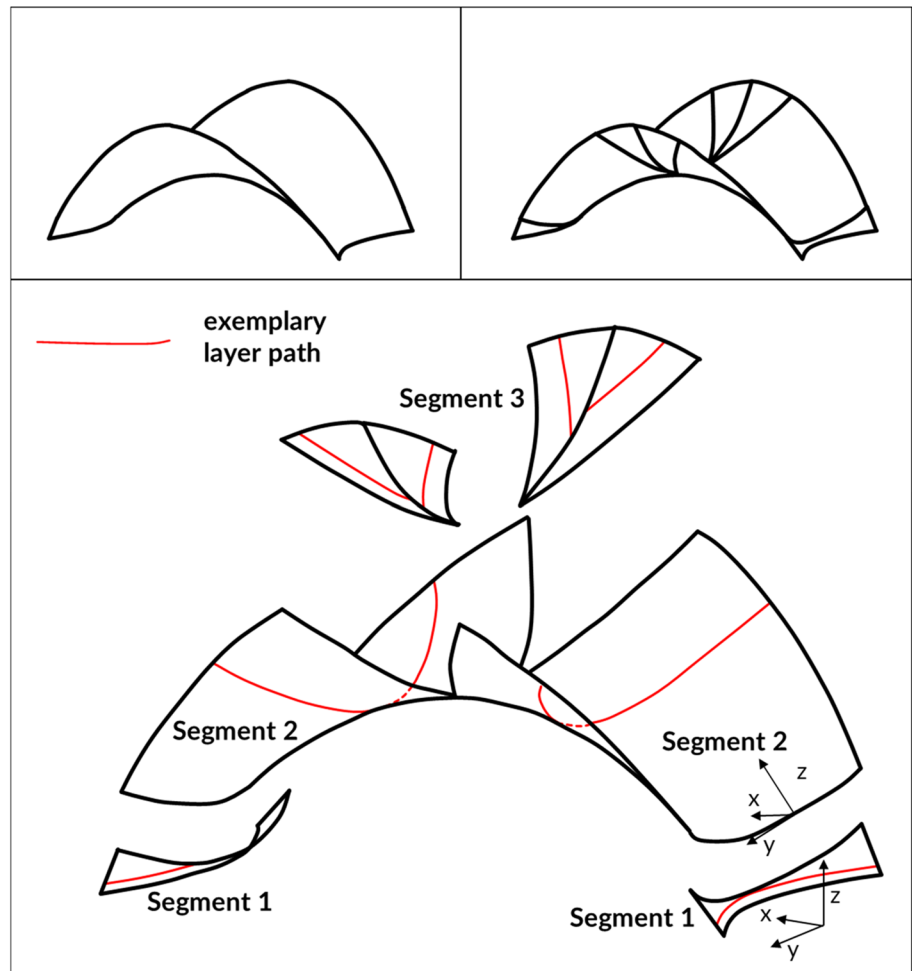**Fig. 19** Segmentation of the bridge model with layered construction

Fig. 20 Scaled bridge model (span approx. 30 cm)

regression, as described above for parametric robot programming. First, segment 1 was manufactured. The welding paths for single layers of each segment are described by the red lines in Fig. 19. The end edge of segment 1 was then inclined by 45° and serves as the basis for the second and third segment, whose coordinate systems are rotated by 45°.

3.3 Process parameters

For the bridge, WAAM parameters were developed at TU Darmstadt, which enable the manufacturing of cantilevered structures without the liquid weld metal dripping down. The possibility of manufacturing overhangs and applying material sideways is the essential aspect and absolutely necessary for being able to manufacture a bridge on site. The usually decisive parameters (travel speed v_s, wire feed speed v_d) and the CMT process regulation (Fronius et al. 2013), therefore, were supplemented by a further parameter, in particular a defined pause length. A determined ratio of CMT cycles and pause time allows the drop to harden sufficiently so that its geometry is no longer significantly influenced by the following drop. The process and input parameters used are listed in Feucht et al. (2020a). The process parameters can be edited via a Fronius CMT Advanced 4000 R power source in the "CMT Cycle Step" characteristic. Further investigations, including on strength and material properties, are described in Feucht et al. (2020b).

The manufacturing strategy and manufacturing parameters were tested on a 1:8 scale model (Fig. 20).

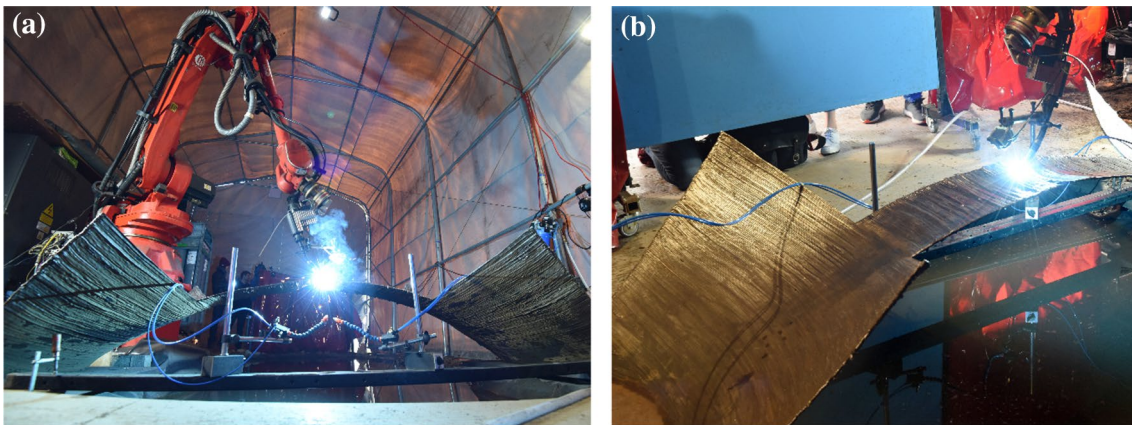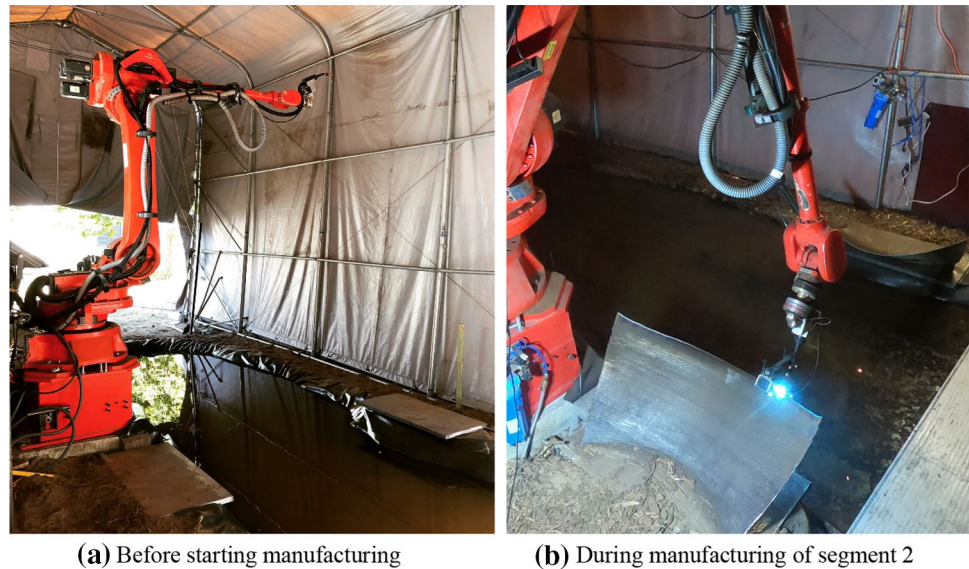**(a)** Before starting manufacturing   **(b)** During manufacturing of segment 2

Fig. 22 Pictures from construction site © Claus Völker

3.4 In situ manufacturing

The knowledge gained in the preliminary investigations described above was used for the manufacturing of the bridge on site. The same robot code was used for the 1:1 scale bridge as for the 1:8 scale model.

In September 2019, the six-axis welding robot with controller, welding equipment, gas and wire was installed directly at a creek on the campus of the TU Darmstadt. To protect inconsiderate passers-by from looking into the arc on the one hand, and to ensure the undisturbed flow of shielding gas on the other, the construction site was enclosed by a tent. Two base plates were connected on Spinnanker foundation anchor heads (concreteless foundation technology),[4] see Fig. 21a.

The first welding layers were then applied and the first segment was manufactured according to the manufacturing strategy. The construction progress during the manufacturing of segment 2 is shown in Fig. 21b.

In mid-October during the manufacturing process, unexpected significant deformations due to thermally induced residual stress occurred. The cross section twisted continuously after the application of only one layer so strongly that the welding robot partially missed the bridge when manufacturing the next layer. This phenomenon has already been described in Table 1, row 3. Thus, the manufacturing strategy was adjusted from the halfway point by dividing the bridge cross section into five strips. First, the middle strip was started (Fig. 22) and with this the bridge was finished by end of October 2019.

Figure 23 pictures the cleared construction site at the end of October 2019. In addition, the picture shows further

---

[4] https://www.spinnanker.com.

Fig. 23 Bridge shortly before being disassembled

cross-sectional zones that were produced after the bridge was closed before clearing the construction site. Final completion is pending.

4 Summary and conclusions

The use of additive manufacturing for applications in the construction industry is currently the focus of much research. Whether steel, concrete or clay: many materials are the subject of investigations. Robots are mostly used to guide the print head, due to the comparatively long range and the possibility of use regardless of location. This article focuses on the additive manufacturing of steel with the wire + arc additive manufacturing. The parametric robot programming offers the possibility to manufacture structures without an exact prediction of the layer geometry. Only the actual layer height must be measured (or checked, depending on the quality of the prediction), which is possible with simple methods (e.g., touch sensing) and is done within the robot controller. The principle of PRP is transferable to any robot manufacturer and allows flexible manufacturing without a direct link between slicing and process monitoring.

The workflow of the PRP is explained in detail. Complex structures can be described using linear regression by mathematical polynomial functions that depend on the variable z. First the geometry is divided into iso-curves. Iso-curves that have more than one x- or y-coordinate for a z value cannot be used. Checking the generated polynomial functions with an independent program (e.g., MATLAB) has proven to be helpful. The robot can then use the polynomial functions to move to the x- and y-coordinates via FOR loops over z and apply the material accordingly. The workflow was presented using shells. However, a transfer to solids is conceivable.

Advantages of the parametric robot programming are as follows:

- Automatic calculation of coordinates for each z-coordinate.
- Short and clear program code.
- Small required memory capacity of the robot.
- Fast reaction in case of deviations between nominal and actual geometry.
- Easy up- and down-scaling of all objects.

The software used in the described workflow (Rhino3D, Grasshopper, MATLAB, etc.) was chosen because it seemed the most suitable. Using other software is possible. It can also be useful to develop a stand-alone system that automates the links between the various software. However, the authors only intended to describe the principle of PRP, so that other users can adapt it for their own purposes, regardless of the robot brand used or the selected print material.

At TU Darmstadt, a pedestrian bridge made of steel was printed in situ using WAAM. The parametric robot programming in conjunction with the manufacturing strategy and process parameters presented in this article make it possible to additively manufacture such cantilevered curved structures.

Compliance with ethical standards

Conflict of interest On behalf of all authors, the corresponding author states that there is no conflict of interest.

References

3DPriyol (2020) Form adaptive joint and pavilion. https://www.3dpriyol.com/project/form-adaptive-joint-pavilion/. Accessed 26 Mar 2020

Almeida PMS (2012) Process control and development in wire and arc additive manufacturing. Cranfield University School of Applied Sciences, Cranfield

Bandari YK, Williams S, Ding J, Martina F (2015) Additive manufacture of large structures: robotic or CNC systems? In: 26th international solid freeform fabrication symposium

Bergmann JP, Henckell P, Reinmann J, Hildebrand J, Ali Y (2018) Grundlegende wissenschaftliche Konzepterstellung zu bestehenden Herausforderungen und Perspektiven für die Additive Fertigung mit Lichtbogen. DVS Media GmbH, Düsseldorf

Borg Costanzi C (2020) BE-AM blog. https://www.public.tableau.com/profile/chris.borg.costanzi#!/vizhome/shared/B3MWGXNQ8. Accessed 26 Mar 2020

Bos F, Wolfs R, Ahmed Z, Salet T (2016) Additive manufacturing of concrete in construction: potentials and challenges of 3D concrete printing. Virtual Phys Prototyp 11(3):209–225

Brandt S (2014) Data analysis statistical and computational methods for scientists and engineers. Springer International Publishing, Cham

Buchanan C, Gardner L (2019) Metal 3D printing in construction: a review of methods, research, applications, opportunities and challenges. Eng Struct 180(2):332–348

Buswell RA, Leal de Silva WR, Jones SZ, Dirrenberger J (2018) 3D printing using concrete extrusion: a roadmap for research. Cem Concr Res 112:37–49

de Witte D, Fehlhaber T (2019) 3D-clay printing—next generation brickwork. CFI Ceram Forum Int 4–5(96):E54–E59

Ding D, Pan Z, Cuiuri D, Li H (2014) A tool-path generation strategy for wire and arc additive manufacturing. Int J Adv Manuf Technol 73(1–4):173–183

Federal Ministry for Economic Affairs (2020) Industrie 4.0. https://www.bmwi.de/Redaktion/EN/Dossier/industrie-40.html. Accessed 26 Mar 2020

Feucht T, Lange J, Waldschmitt B, Schudlich A-K, Klein M, Oechsner M (2020a) Welding process for the additive manufacturing of cantilevered components with the WAAM. In: da Silva LFM, Martins PAF, El-Zein MS (eds) Advanced joining processes. Springer, Singapore

Feucht T, Waldschmitt B, Lange J, Erven M (2020) 3D-printing with steel: additive manufacturing of a bridge in situ. In: Proceedings of the EuroSteel conference 2020

Fronius, Bruckner J, Egerland S, Himmelbauer K, Millinger A, Schörghuber M, Söllinger D, Waldhör A (2013) Schweißpraxis aktuell: CMT-Technologie. Cold Metal Transfer—ein neuer Metall-Schutzgas-Schweißprozess. WEKA MEDIA GmbH & Co. KG, Kissing

International Federation of Robotics (2013) World robotics 2013 industrial robots. International Federation of Robotics, Frankfurt am Main

International Federation of Robotics (2020) FACTS about ROBOTS—worldwide. https://www.ifr.org/ifr-press-releases/news/facts-about-robots-worldwide. Accessed 26 Mar 2020

John F, Fischer G, Armatys K, Riemann A, Röhrich T (2017) Potentiale von drahtbasierten Lichtbogenprozessen für die additive Fertigung. In: Mayr P, Berger M (eds) Füge- und Montagetechnik Chemnitz. Universitätsverlag Chemnitz, Chemnitz

Knaack U, Tessmann O, Bilow M, de Witte D (2017) Imagine 10—Rapids 02. Nai010 Publishers, Rotterdam

Lasi H, Fettke P, Kemper H-G, Feld T, Hoffmann M (2014) Industry 4.0. Bus Inf Syst Eng 6(4):239–242

Ma G, Wang L, Ju Y (2018) State-of-the-art of 3D printing technology of cementitious material—an emerging technique for construction. Sci China Technol Sci 61(4):475–495

Martina F, Williams S (2015) Wire + arc additive manufacturing vs. traditional machining from solid: a cost comparison. Cranfield University, Cranfield

Math.NET Numcerics (2020) Math.NET Numcerics. https://www.numerics.mathdotnet.com. Accessed 26 Mar 2020

Mechtcherine V, Grafe J, Nerella VN, Spaniol E, Hertel M, Füssel U (2018) 3D-printed steel reinforcement for digital concrete construction—manufacture, mechanical properties and bond behaviour. Constr Build Mater 179(2018):125–137

MX3D (2020) https://www.mx3d.com/. Accessed 26 Mar 2020

Seel M, Akerboom R, Knaack U, Oechsner M, Hof P, Schneider J (2018) Fused glass deposition modelling for applications in the built environment. Materialwiss Werkstofftech 49(7):870–880

Strauß H (2013) AM envelope—the potential of additive manufacturing for facade construction. CreateSpace Independent Publishing Platform, Delft

TU Ilmenau (2020) FG Fertigungstechnik. https://www.tu-ilmenau.de/fertigungstechnik/. Accessed 26 Mar 2020

Vogel Communications Group (2020) Market study on the current status of industrial 3D printing. https://www.mission-additive.de/the-current-status-of-industrial-3d-printing-d-42477/. Accessed 26 Mar 2020

Zhang YM, Li P, Chen Y, Male AT (2002) Automated system for welding-based rapid prototyping. Mechatronics 12:37–53